Inorg. Chem. **2003**, *42*, 8534–8544

Inorganic Chemistry

Article

Ligand Effect on Reversible Conversion between Copper(I) and Bis(μ-oxo)dicopper(III) Complex with a Sterically Hindered Tetradentate Tripodal Ligand and Monooxygenase Activity of Bis(μ-oxo)dicopper(III) Complex

Masayasu Mizuno,[†] Hideki Hayashi,[†] Shuhei Fujinami,[†] Hideki Furutachi,[†] Shigenori Nagatomo,[‡] Shigenori Otake,[†] Kounosuke Uozumi,[†] Masatatsu Suzuki,[†,*] and Teizo Kitagawa[‡,*]

Department of Chemistry, Faculty of Science, Kanazawa University, Kakuma-machi, Kanazawa 920-1192, Japan, and Center for Integrative Bioscience, Okazaki National Research Institutes, Myodaiji, Okazaki, 444-8585 Japan

Received May 14, 2003

A new sterically hindered tetradentate tripodal ligand (Me_2-etpy) and its labeled analogue having deuterated methylene groups (d_4-Me_2-etpy) were synthesized, where Me_2-etpy is bis(6-methyl-2-pyridylmethyl)(2-pyridylethyl)amine. Copper(I) complexes [Cu(Me_2-etpy or d_4-Me_2-etpy)]$^+$ (**1** and **1**-d_4, respectively) reacted with dioxygen at –80 °C in acetone to give bis(μ-oxo)dicopper(III) complexes [$Cu_2(O)_2$(Me_2-etpy or d_4-Me_2-etpy)$_2$]$^{2+}$ (**1**-oxo and **1**-d_4-oxo, respectively), the latter of which was crystallographically characterized. Unlike a bis(μ-oxo)dicopper(III) complex with a closely related Me_2-tpa ligand having a 2-pyridylmethyl pendant, **1**-oxo possessing a 2-pyridylethyl pendant is not fully formed even under 1 atm of O_2 at –80 °C and is very reactive toward the oxidation of the supporting ligand. Thermal decomposition of **1**-oxo gave an *N*-dealkylated ligand in yield ~80% based on a dimer and a corresponding aldehyde. The deuterated ligand d_4-Me_2-etpy greatly stabilizes the bis(μ-oxo)dicopper(III) complex **1**-d_4-oxo, indicating that the rate determining step of the *N*-dealkylation is the C–H bond cleavage from the methylene group. The reversible conversion between **1**-d_4 and **1**-d_4-oxo in acetone is dependent on the temperature, and the thermodynamic parameters (ΔH and ΔS) of the equilibrium were determined to be -53 ± 2 kJ mol^{-1} and -187 ± 10 J mol^{-1} K^{-1}, respectively. The effect of the 2-pyridylethyl pendant in comparison with the 2-pyridylmethyl and 6-methyl-2-pyridylmethyl pendants on the physicochemical properties of the copper(I) and bis(μ-oxo)dicopper(III) species is discussed.

Introduction

Dioxygen activation chemistry by dicopper complexes is of current interest for understanding the reaction mechanisms of dioxygen activating dicopper proteins in biological systems and utilizing metal complexes as oxidation catalysts. Various types of synthetic $Cu_2{-}O_2$ complexes have been developed by tuning the coordination environments.[1−7] A variety of tetradentate tripodal ligands have been designed for modulating the stereochemical and electronic nature of copper(I) and copper(II) complexes. Karlin and co-workers have demonstrated that a copper(I) complex having a tetradentate tripodal ligand TMPA,[8] [Cu(TMPA)($NCCH_3$)]$^+$ (**2**), reacts with O_2 to form a *trans*-(μ-1,2-peroxo)dicopper(II) complex ([$Cu_2(O_2)(TMPA)_2$]$^{2+}$ (**2**-O_2)) in a trigonal bipyramidal structure.[9] Previously, we found that introduction of 6-methylpyridyl group(s) instead of the pyridyl group(s) of TMPA ligand shown in Scheme 1 has a significant influence on the dioxygen reactivity of the copper(I) complexes and the nature of the oxygenated species: the

---

[*] To whom correspondence should be addressed. E-mail: suzuki@cacheibm.s.kanazawa-u.ac.jp (M.S.); teizo@ims.ac.jp (T.K.). Phone: +81-76-264-5701 (M.S.). Fax: +81-76-264-5742 (M.S.).

[†] Kanazawa University.

[‡] Okazaki National Research Institutes.

(1) Kitajima, N.; Moro-oka, Y. *Chem. Rev.* **1994**, *94*, 737.

(2) Karlin, K. D.; Zuberbühler, A. D. In *Bioinorganic Catalysis*, 2nd ed.; Reedijk, J., Bouwman, E., Eds.; Marcel Dekker: New York, 1999; p 469.

(3) Tolman, W. B. *Acc. Chem. Res.* **1997**, *30*, 227.

(4) Holland, P. L.; Tolman, W. B. *Coord. Chem. Rev.* **1999**, *190−192*, 855.

(5) Solomon, E. I.; Chen, P.; Metz, M.; Lee, S.-K.; Palmer, A. E. *Angew. Chem., Int. Ed.* **2001**, *40*, 4570.

(6) Que, L., Jr.; Tolman, W. B. *Angew. Chem., Int. Ed.* **2002**, *41*, 1114.

(7) Itoh, S.; Fukuzumi, S. *Bull. Chem. Soc. Jpn.* **2002**, *75*, 2081.

10.1021/ic0345166 CCC: $25.00

Scheme 1. Tetradentate Tripodal Ligands and Their Reactivity

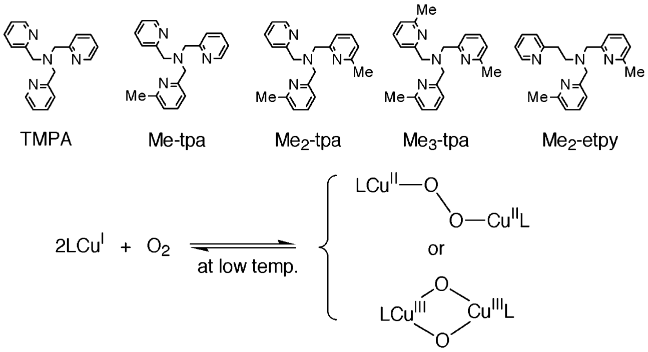

reaction of $[Cu(Me\text{-}tpa)]^+$ (**3**) with O_2 generates a *trans*-(*μ*-1,2-peroxo)dicopper(II) species,[10] whereas $[Cu(Me_2\text{-}tpa)]^+$ (**4**) and $[Cu(d_{15}\text{-}Me_3\text{-}tpa)]^+$ (**5**-d_{15}) produce bis(*μ*-oxo)dicopper(III) species $[Cu_2(O)_2(Me_2\text{-}tpa)_2]^{2+}$ (**4**-oxo) and $[Cu_2(O)_2(d_{15}\text{-}Me_3\text{-}tpa)_2]^{2+}$ (**5**-d_{15}-oxo) upon oxygenation, respectively,[11,12] where d_{15}-Me_3-tpa is a labeled analogue having the perdeuterated methyl and methylene groups. Thus, introduction of more than two 6-methylpyridyl groups into TMPA ligand prevents the formation of *trans*-(*μ*-1,2-peroxo)dicopper(II) species in a trigonal bipyramidal structure, probably due to a steric requirement of 6-methylpyridyl groups.

It has been shown that some sterically hindered bidentate and tridentate ligands form (μ-η^2:η^2-peroxo)dicopper(II) and/or bis(*μ*-oxo)dicopper(III) complexes.[13−18] Tolman and coworkers first demonstrated that some (μ-η^2:η^2-peroxo)dicopper(II) complexes having sterically hindered tridentate *N*,*N*′,*N*″-trisubstitued tacn undergo facile interconversion with bis(*μ*-oxo)dicopper(III) species.[15a] Furthermore, in certain instances, monooxygenase activity of bis(*μ*-oxo)dicopper(III) species have been reported. The relative stability between (μ-η^2:η^2-peroxo)dicopper(II) and bis(*μ*-oxo)dicopper(III) species depends on various factors such as electronic and steric effects as well as solvents, counterion, temperature, and so on.[15a,19−23] As mentioned above, we have also found that the complex **4**-oxo is reversibly converted to copper(I) precursors by bubbling of nitrogen gas. The equilibrium involves a reversible four-electron redox process between copper(I) and O_2. Thus, it is interesting to explore how the nature of a series of sterically hindered tetradentate tripodal ligands which can modulate the electronic and stereochemical effects, especially redox properties, influences the relative stability of those three species, and reactivity of bis(*μ*-oxo)dicopper(III) species. In this study, we report the syntheses of new copper(I) and bis(*μ*-oxo)dicopper(III) complexes having a sterically hindered tetradentate tripodal ligand, bis(6-methyl-2-pyridylmethyl)(2-pyridylethyl)amine, Me_2-etpy, or its labeled analogue having deuterated methylene groups, and their physicochemical properties in comparison with those of the closely related complexes $[Cu(Me_2\text{-}tpa)]^+$ (**4**) and $[Cu(Me_3\text{-}tpa\text{ or }d_{15}\text{-}Me_3\text{-}tpa)]^+$ (**5** and **5**-d_{15}).

Experimental Section

Materials. All reagents and solvents were obtained from commercial sources and used without further purification except for ligand recovering experiments and spectroscopic measurements. Acetone used for these experiments was dried by molecular sieves 5A and was distilled under N_2 atmosphere.

Syntheses of Ligands. Bis(6-methyl-2-pyridylmethyl)(2-pyridylethyl)amine (Me_2-etpy). A methanol solution (50 cm^3) of 2-(2-aminoethyl)pyridine (10.0 g, 81.9 mmol) was added to a methanol solution (50 cm^3) of 6-methylpyridine-2-aldehyde (20.1 g, 166 mmol) and acetic acid (4.5 g, 150 mmol). To the resulting cold solution was slowly added $NaBH_3CN$ (8.29 g, 132 mmol) with stirring at room temperature. After stirring for 3 days, concentrated hydrochloric acid was added to the mixture to decompose excess $NaBH_3CN$ until the pH became 1 (HCN gas evolved was trapped and decomposed by 10% sodium hypochlorite solution). The solution was stirred for 1 day and was concentrated almost to dryness under reduced pressure. The residue was dissolved into an

---

(8) Abbreviations of ligands used: TMPA = tris(2-pyridylmethyl)amine; Me_2-etpy = bis(6-methyl-2-pyridylmethyl)(2-pyridylethyl)amine; Me-tpa = bis(2-pyridylmethyl)(6-methyl-2-pyridylmethyl)amine; Me_2-tpa = bis(6-methyl-2-pyridylmethyl)(2-pyridylmethyl)amine; Me_3-tpa = tris(6-methyl-2-pyridylmethyl)amine; pmea = bis(2-pyridylmethyl)-(2-pyridylethyl)amine; Bn_3-tacn = 1,4,7-tribenzyl-1,4,7-triazacyclononane; $^iPr_3$-tacn = 1,4,7-*iso*-propyl-1,4,7-triazacyclononane; L_{ME} = *N*,*N*′-dimethyl-*N*,*N*′-diethylcyclohexanediamine; AN = 3,3′-iminobis(*N*,*N*-dimethylpropylamine); MeAN = *N*,*N*,*N*′,*N*′,*N*″-pentamethyldipropylenetriamine; HB(3,5-R_2pz)$_3$ = hydrotris(3,5-dialkyl-1-pyrazolyl)borate; R-XTL-H = *N*,*N*,*N*′,*N*′-tetra(2-pyridylethyl)-1,3-diaminoxylene; TMQA = tri(2-quinolylmethyl)amine; Ph_3tren = tri(4-phenyl-3-aza-3-butenyl)amine.

(9) (a) Jacobson, R. R.; Tyeklár, Z.; Farooq, A.; Karlin, K. D.; Liu, S.; Zubieta, J. *J. Am. Chem. Soc.* **1988**, *110*, 3690. (b) Tyeklár, Z.; Jacobson, R. R.; Wei, N.; Murthy, N. N.; Zubieta, J.; Karlin, K. D. *J. Am. Chem. Soc.* **1993**, *115*, 2677.

(10) Uozumi, K.; Hayashi, Y.; Suzuki, M.; Uehara, A. *Chem. Lett.* **1993**, 963.

(11) Hayashi, H.; Fujinami, S.; Nagatomo, S.; Ogo, S.; Suzuki, M.; Uehara, A.; Watanabe, Y.; Kitagawa, T. *J. Am. Chem. Soc.* **2000**, *122*, 2124.

(12) Hayashi, H.; Uozumi, K.; Fujinami, S.; Nagatomo, S.; Shiren, K.; Furutachi, H.; Suzuki, M.; Uehara, A.; Kitagawa, T. *Chem. Lett.* **2002**, 416.

(13) Kitajima, N.; Fujisawa, K.; Fujimoto, C.; Moro-oka, Y.; Hashimoto, S.; Kitagawa, T.; Toriumi, K.; Tatsumi, K.; Nakamura, A. *J. Am. Chem. Soc.* **1992**, *114*, 1277.

(14) Kodera, M.; Katayama, K.; Tachi, Y.; Kano, K.; Hirota, S.; Fujinami, S.; Suzuki, M. *J. Am. Chem. Soc*. **1999**, *121*, 11006.

(15) (a) Halfen, J. A.; Mahapatra, S.; Wilkinson, E. C.; Kaderli, S.; Young, V. G., Jr.; Que, L., Jr.; Zuberbühler, A. D.; Tolman, W. B. *Science* **1996**, *271*, 1397. (b) Mahapatra, S.; Halfen, J. A.; Wilkinson, E. C.; Pan, G.; Wang, X.; Young, V. G., Jr.; Cramer, C. J.; Que, L., Jr.; Tolman, W. B. *J. Am. Chem. Soc.* **1996**, *118*, 11555. (c) Mahapatra, S.; Halfen, J. A.; Tolman, W. B. *J. Am. Chem. Soc.* **1996**, *118*, 11575.

(16) Mahadevan, V.; Hou, Z.; Cole, A. P.; Root, D. E.; Lal, T. K.; Solomon, E. I.; Stack, T. D. P. *J. Am. Chem. Soc.* **1997**, *119*, 11996.

(17) (a) Obias, H. V.; Lin, Y.; Murthy, N. N.; Pidcock, E.; Solomon, E. I.; Ralle, M.; Blackburn, N. J.; Neuhold, Y.-M.; Zuberbühler, A. D.; Karlin, K. D. *J. Am. Chem. Soc.* **1998**, *120*, 12960. (b) Pidcock, E.; DeBeer, S.; Obias, H. V.; Hedman, B.; Hodgson, K. O.; Karlin, K. D.; Solomon, E. I. *J. Am. Chem. Soc.* **1999**, *121*, 1870.

(18) Cvetkovic, M.; Batten, S. R.; Moubaraki, B.; Keith, S.; Murray, K. S.; Spiccia, L. *Inorg. Chim. Acta* **2001**, *324*, 131.

(19) (a) Mahapatra, S.; Kaderli, S.; Llobet, A.; Neuhold, Y.-M.; Palanché, T.; Halfen, J. A.; Young, V. G., Jr.; Kaden, T. A.; Que, L., Jr.; Zuberbühler, A. D.; Tolman, W. B. *Inorg. Chem.* **1997**, *36*, 6343. (b) Cahoy, J.; Holland, P. L.; Tolman, W. B. *Inorg. Chem.* **1999**, *38*, 2161. (c) Lam, B. M. T.; Halfen, J. A.; Young, V. G., Jr.; Hagadorn, J. R.; Holland, P. L.; Lledós, A.; Cucurull-Sánchez, L.; Novoa, J. J.; Alvarez, S.; Tolman, W. B. *Inorg. Chem.* **2000**, *39*, 4059.

(20) Mahadevan, V.; Henson, M. J.; Solomon, E. I.; Stack, T. D. P. *J. Am. Chem. Soc.* **2000**, *122*, 10249.

(21) Liang, H.-C.; Zhang, C. X.; Henson, M. J.; Sommer, R. D.; Hatwell, K. R.; Kaderli, S.; Zuberbühler, A. D.; Rheingold, A. L.; Solomon, E. I.; Karlin, K. D. *J. Am. Chem. Soc.* **2002**, *124*, 4170.

(22) Taki, M.; Teramae, S.; Nagatomo, S.; Tachi, Y.; Kitagawa, T.; Itoh, S.; Fukuzumi, S. *J. Am. Chem. Soc.* **2002**, *124*, 6367.

(23) Mirica, L. M.; Vance, M.; Rudd, D. J.; Hedman, B.; Hodgson, K. O.; Solomon, E. I.; Stack, T. D. P. *J. Am. Chem. Soc.* **2002**, *124*, 9332.

aqueous NaOH solution (100 cm^3) and extracted with chloroform (3 × 50 cm^3). The combined extracts were dried over Na_2SO_4 and evaporated under reduced pressure to give an orange oil, which was dissolved into hot hexane (300 mL), and insoluble material was removed by decantation three times. The resulting hexane solution was concentrated under reduced pressure to give a yellow oil. Yield: 12.3 g (45%). Further purification was achieved by silica gel column chromatography with methanol/chloroform (l.3% $CH_3OH/CHCl_3$). ^1H NMR ($CDCl_3$, 400 MHz): δ(ppm) = 2.51 (6H, s, CH_3), 3.00 (4H, m, CH_2CH_2), 3.86 (4H, s, CH_2), 6.97 (2H, d, pyH), 7.10 (1H, m, et-pyH), 7.17 (2H, d, pyH), 7.46 (2H, t, pyH), 7.55 (2H, t, et-pyH), 8.47 (1H, m, et-pyH). ^{13}C NMR ($CDCl_3$, 100 MHz): δ (ppm) = 24.1 (CH_3), 35.8 (NCH_2CH_2py), 54.2 (NCH_2CH_2py), 60.2 (CH_2), 119.2 (py), 120.7 (py), 121.0 (py), 123.2 (py), 135.7 (py), 136.3 (py), 148.8 (py), 157.1 (py), 159.1 (py), 160.4 (py). FAB-MS: *m*/*z* 333 $[MH]^+$.

6-Methylpicolinic Acid Methyl Ester. Thionyl chloride (23.8 g, 200 mmol) was added dropwise to 6-methylpicolinic acid (7.02 g, 51.2 mmol) in ice bath with stirring. The reaction mixture was stirred for 4 h at 40 °C, and an excess amount of thionyl chloride was removed under reduced pressure to give an oil, to which was added methanol (ca. 150 mL), and the resulting solution was stirred for 1 day. Evaporation of methanol yielded a purple oil. The oil was washed with diethyl ether several times to give a purple solid of 6-methylpicolinic acid methyl ester hydrochloride, which was dissolved into an aqueous potassium carbonate to neutralize. 6-Methylpicolinic acid methyl ester was extracted with $CHCl_3$ (3 × 50 cm^3). The combined extracts were dried over Na_2SO_4 and concentrated under reduced pressure to give 6-methylpicolinic acid methyl ester (7.7 g). Yield was almost quantitative. ^1H NMR ($CDCl_3$, 400 MHz): δ(ppm) = 2.66 (3H, s, CH_3), 4.00 (3H, s, CH_3(ester)), 7.36 (1H, d, pyH), 7.75 (1H, t, pyH), 7.94 (1H, d, pyH).

6-Methylpyridine-2-methanol-*d*$_2$. 6-Methylpicolinic acid methyl ester (7.56 g, 50 mmol) was dissolved into ca. 100 mL of dry EtOH. $NaBD_4$ (8.37 g, 200 mmol) was added slowly to the cold solution in an ice bath. After stirring for 3 days, HCl was added until pH of the solution became 1 to decompose an excess of $NaBD_4$. An aqueous solution of NaOH was added to make the solution basic, and the solution was concentrated under reduced pressure to remove EtOH at room temperature. The resulting solution was extracted with chloroform (3 × 100 cm^3). The combined extracts were dried over Na_2SO_4, and chloroform was removed by evaporation under reduced pressure at room temperature to give yellow liquid of 6-methylpyridine-2-methanol-*d*$_2$. Yield: 4.36 g (70%). ^1H NMR ($CDCl_3$, 400 MHz): δ(ppm) = 2.55 (3H, s, CH_3), 3.83 (1H, s, OH), 7.03 (2H, m, pyH), 7.59 (1H, t, pyH). ^{13}C NMR ($CDCl_3$, 100 MHz): δ(ppm) = 23.8 (CH_3), 63.4 (CD_2, quintet), 117.6, 121.7 (3- or 5-py), 136.9 (4-py), 157.2, 158.8 (2- or 6-py). ESI-MS (methanol solution containing a small amount of formic acid): *m*/*z* 126 $[MH]^+$.

***d*$_4$-Me$_2$-etpy.** To a $CHCl_3$ solution (50 mL) of 6-methylpyridine-2-methanol-*d*$_2$ (1.38 g, 11 mmol) was added dropwise thionyl chloride (4.76 g, 40 mmol) with stirring in an ice bath. The solution was heated at 50 °C for 5 h. Chloroform and the excess of thionyl chloride were removed by evaporation under reduced pressure to yield a white powder. The powder obtained was dissolved into water (50 mL), to which was added 2-(2-aminoethyl)pyridine (0.672 g, 5.5 mmol), and then the pH of the mixture was adjusted to 10. The solution was stirred for 3 days, in which the pH was maintained to 10. NaOH was added to the resulting solution, and the oily layer was extracted with $CHCl_3$ (3 × 25 mL). The combined extracts were dried over Na_2SO_4, and chloroform was removed by evaporation under reduced pressure to give an orange-brown oil of *d*$_4$-Me$_2$-etpy, which was used without further purification. Yield: 1.80 g (97%). ^1H NMR ($CDCl_3$, 400 MHz): δ(ppm) = 2.51 (6H, s, CH_3), 2.98 (4H, m, CH_2CH_2), 6.95 (2H, d, pyH), 7.09 (1H, m, et-pyH), 7.16(2H, d, pyH), 7.45 (2H, t, pyH), 7.55(2H, t, et-pyH), 8.48 (1H, m, et-pyH). ESI-MS (methanol solution containing a small amount of formic acid): *m*/*z* 337 $[MH]^+$.

Syntheses of Complexes. Copper(I) and copper(II) complexes were prepared under N_2 atmosphere using Schlenk techniques. [Cu(TMPA)(CH_3CN)]ClO_4 (**2**)[9] and [Cu(Me-tpa)]$ClO_4\cdot 0.5H_2O$ (**3**)[10] were synthesized by the literature methods. *Caution: Perchlorate salts are potentially explosive and should be handled with care.*

[Cu(Me$_2$-etpy)]ClO$_4$ (1·ClO$_4$). An ethanol solution (20 mL) of Me$_2$-etpy (733 mg, 2.2 mmol) was added to $[Cu(CH_3CN)_4]ClO_4$ (622 mg, 1.9 mmol). The resulting suspension was dissolved by heating to give a yellow solution which was allowed to stand overnight to yield dark yellow crystals, which were collected by filtration, washed with ether, and dried in vacuo. Recrystallization from MeOH (20 mL) gave yellow crystals suitable for X-ray crystallography. Yield: 580 mg (62%). Anal. Calcd for $CuC_{21}H_{24}N_4ClO_4$: C, 50.91; H, 4.88; N, 11.31%. Found: C, 50.72; H, 4.80; N, 11.37%. IR (KBr, cm^{-1}): 1599 (C=C, aromatic), 1574, 1464, 1442, 1090 (ClO_4^-), 787, 624 (ClO_4^-). ESI-MS (acetonitrile solution): *m*/*z* 395 $[M]^+$.

[Cu(*d*$_4$-Me$_2$-etpy)]ClO$_4$ (1-*d*$_4$·ClO$_4$). This was synthesized by the same method as **1**·ClO_4. Anal. Calcd for $CuC_{21}H_{20}D_4N_4ClO_4$: C, 50.50; H/D, 4.84; N, 11.22%. Found: C, 50.23; H/D, 4.90; N, 11.07%. ^1H NMR (d_6-acetone, −80 °C, 400 MHz): δ(ppm) = 3.02 (6H, s, CH_3), 3.19 (2H, s(broad), CH_2CH_2), 3.29 (2H, s(broad), CH_2CH_2), 7.44 (2H, d, pyH), 7.50 (2H, d, et-pyH), 7.56 (2H, d, pyH), 7.91 (2H, t, pyH), 7.98 (1H, t, et-pyH), 9.17 (1H, m, et-pyH). ESI-MS (acetonitrile solution): *m*/*z* 399 $[M]^+$.

[Cu$_2$(O)$_2$(*d*$_4$-Me$_2$-etpy)$_2$](ClO$_4$)$_2$·7(CH$_3$)$_2$CO (1-*d*$_4$-oxo·ClO$_4$). To an acetone solution (3 mL) of **1**-*d*$_4$·ClO_4 (ca. 45 mg) was injected O_2 at −80 °C. To the resulting brown solution was added *n*-hexane (0.4 mL), and the solution was allowed to stand at −80 °C for a few days to afford orange-brown crystals suitable for X-ray crystallography. ^1H NMR (d_6-acetone, −80 °C, 400 MHz): δ(ppm) = 1.22 (3H, s, CH_3), 1.82 (3H, s, CH_3), 2.36 (1H, m, CH_2CH_2), 2.80 (1H, m, CH_2CH_2), 2.88 (1H, d, CH_2CH_2), 3.08 (1H, d, CH_2CH_2), 7.18 (2H, m, pyH), 7.33 (1H, d, pyH). The signals that appeared in the lower field region could not be identified because of overlapping with those of **1**-*d*$_4$·ClO_4 present in the solution (vide infra).

[Cu$_2$(Me$_2$-etpy)$_2$(OMe)$_2$](ClO$_4$)$_2$·3H$_2$O (1-OMe·ClO$_4$). To a methanol solution (50 mL) of $Cu(ClO_4)_2\cdot 6H_2O$ (760 mg, 2 mmol) was added Me$_2$-etpy (665 mg, 2 mmol), to which was added triethylamine (202 mg, 2 mmol) with stirring. The resulting suspension was dissolved by heating to give a green solution which was allowed to stand overnight to afford green crystals, which were collected by filtration, washed with ether, and dried in vacuo. Yield: 530 mg (48%). Anal. Calcd for $Cu_2C_{44}H_{60}N_8Cl_2O_{13}$: C, 47.74; H, 5.46; N, 10.12%. Found: C, 47.77; H, 5.04; N, 10.29%. IR (KBr, cm^{-1}): 1606 (C=C, aromatic), 1577, 1465, 1444, 1091 (ClO_4^-), 791, 625 (ClO_4^-). UV−vis (acetone): λ_{max} = 642 nm (ϵ = 260 M^{-1} cm^{-1}). ESI-MS (acetonitrile solution): *m*/*z* 395 $[M/2 - OCH_3]^+$, and 426 $[M/2]^+$. The complex was also obtained by thermal decomposition of **1** in methanol at room temperature under O_2. Single crystals suitable for X-ray analysis were obtained from the methanol solution.

Physical Measurements. The electronic spectra were measured with a Shimadzu diode array spectrometer Multispec-1500 or an Otsuka Electronics photodiode array spectrometer MCPD-2000 with an Otsuka Electronics optical fiber attachment. The temperatures were controlled with a Unisoku thermostated cell holder for the former instrument and with a EYELA low temperature pairstirrer PSL-1800 for the latter one. The reflectance spectra were obtained with an Otsuka Electronics photodiode array spectrometer MCPD-2000 with an Otsuka Electronics optical fiber attachment. The crystalline samples were finely ground and spread on a white filter paper attached on a handmade cold copper plate immersed inside a liquid N_2 Dewar vessel at ∼−110 °C.

Resonance Raman spectra were obtained with a liquid nitrogen cooled CCD detector (model LN/CCD-1340 × 400PB, Princeton Instruments) attached to a 1 m-single polychromator (model MC-100DG, Ritsu Oyo Kogaku). The 406.7 nm line of a Kr^+ laser (model 2060 Spectra Physics) was used as an exciting source. The laser powers used were ∼10 mW at the sample point. All measurements were carried out with a spinning cell (1000 rpm) at ∼−45 to ∼−80 °C. Raman shifts were calibrated with indene, and the accuracy of the peak positions of the Raman bands was ±1 cm^{-1}.

Cyclic voltammograms were obtained with a BAS CV-27 using a three-electrode configuration, including a glassy carbon working electrode, a platinum coil auxiliary electrode, and a saturated Ag/$AgNO_3$ electrode (0.1M *n*-tetrabuthylammonium perchlorate in acetonitrile) as a reference electrode. Acetonitrile was used as a solvent ([Cu] = ∼1 mM) and *n*-tetrabuthylammonium perchlorate (10 mM) as a supporting electrolyte. The $E_{1/2}$ (ΔE) of ferrocene/ferrocenium (Fe^{III}/Fe^{II}) with this setup was 92 mV (96 mV). ^1H NMR spectra were measured with JEOL JNM-LM300 or -LM400. Tetramethylsilane was used as an internal standard. Infrared spectra were obtained by the KBr disk method with a HORIBA FT-200 spectrophotometer. GC-MS analysis was performed on a Shimadzu GCMS-QP5050A GC-MS equipped with a Shimadzu fused silica capillary column HiCap-CBP1-M25-025 (0.22 mm diameter × 25 m). ESI-TOF/MS spectra were measured with a Micromass LCT spectrometer.

Oxygenation (Thermodynamic) Measurement. The equilibrium constant (*K*) of the oxygenation reaction given in eq 1 was estimated by NMR and spectrophotometric measurements in acetone.

$$2[\mathrm{Cu}(d_4\text{-Me}_2\text{-etpy})]^+\ (\mathbf{1}\text{-}d_4) + \mathrm{O}_2 \overset{K}{\rightleftharpoons} [\mathrm{Cu}_2(\mathrm{O})_2(d_4\text{-Me}_2\text{-etpy})_2]^{2+}\ (\mathbf{1}\text{-}d_4\text{-oxo}) \quad (1)$$

$$K = \frac{[\mathbf{1}\text{-}d_4\text{-oxo}]}{[\mathbf{1}\text{-}d_4]^2[\mathrm{O}_2]} \quad (2)$$

First, the equilibrium constant (*K*) at −80 °C was estimated by NMR measurement. The spectrum of an d_6-acetone solution of **1**-d_4 at −80 °C under 1 atm of O_2 showed two sets of signals attributable to **1**-d_4 and **1**-d_4-oxo (vide infra, see Figure 6). The concentrations of **1**-d_4 and **1**-d_4-oxo were determined by the integration of the signals attributable to two species. The average formation ratio of **1**-d_4-oxo was 70% (from two experiments, [Cu] = 19.0 mM and 18.9 mM). The equilibrium constant thus obtained was 4.0×10^4 M^{-2} at −80 °C and the ϵ_{526} value was estimated to be 435 M^{-1} cm^{-1} from the electronic spectrum at −80 °C by using $K = 4.0 \times 10^4$ M^{-2}, which is in good agreement with values obtained from independent electronic spectral measurement given below, where the O_2 concentration was assumed to be 5.106 mM taken from the literature[19a] and the concentration changes of the complex depending on the temperatures were corrected by the following thermal expansion of the solvent (ρ(g/mL) = $-1.1248 \times 10^{-3}T$(K) + 1.1218).[19a]

The equilibrium constant *K* and ϵ_{526} of **1**-d_4-oxo at 526 nm (λ_{max}) at −80 °C were also estimated by fitting the concentration dependence of the electronic spectra by using eq 3, since **1**-d_4-oxo is not fully formed even under 1 atm of O_2 (vide infra).

$$\Delta A_{526} = \frac{\epsilon_{526} \times [(4Ka[\mathrm{O}_2] + 1) - \sqrt{8Ka[\mathrm{O}_2] + 1}]}{8K[\mathrm{O}_2]} \quad (3)$$

In eq 3, *K* and ϵ_{526} are the fitting parameters, ΔA_{526} is difference of the absorbance at 526 nm (λ_{max}) before and after oxygenation, *a* is the initial concentration of **1**-d_4 (2.13, 4.97, 9.33, 9.80 mM at room temperature). The fitting is given in Figure S1 in Supporting Information. The *K* and ϵ_{526} thus obtained are 4.0×10^4 M^{-2} and 437 M^{-1} cm^{-1} at −80 °C, which are in good agreement with those obtained from NMR measurement. *K* values at other temperatures were estimated using ϵ_{526} = 437 M^{-1} cm^{-1}, which were assumed to be constant over the temperature range. The results are given in Table 4. The van't Hoff plot for oxygenation is given in Figure S2 in Supporting Information.

Isolation and Identification of Modified Ligands by Thermal Decomposition of 1-oxo under O_2 Atmosphere. The ligand recovery experiment was performed as follows. Typically, **1** (ca. 100 mg) was dissolved into 20 mL of acetone, and the resulting solution was cooled to −80 °C and exposed to O_2 to produce **1**-oxo. The solution was allowed to stand at −80 °C under O_2 atmosphere until the decomposition was completed (a few days). Evaporation of acetone under reduced pressure yielded a green oil. To this oil was added $CHCl_3$ (20 mL) and concentrated aqueous ammonia (20 mL) with stirring. Organic compounds were extracted with $CHCl_3$ (3 × 20 mL). The combined extracts were dried over Na_2SO_4, and chloroform was removed by evaporation under reduced pressure to give an oil. Me_2-etpy and *N*-dealkylated ligands ((6-methyl-2-pyridylmethyl)(2-pyridylethyl)amine (Me-etpy)) were separated and isolated by TLC ($CHCl_3$/MeOH = 9:1), and they were identified by ^1H NMR and FAB-MS. GC-MS analysis also confirmed the presence of 6-methylpyridine-2-aldehyde together with Me_2-etpy and Me-etpy. ^1H NMR for Me-etpy ($CDCl_3$, 400 MHz): δ(ppm) = 2.51 (3H, s, CH_3), 3.09 (4H, m, CH_2CH_2), 3.93 (2H, s, CH_2), 7.02 (1H, d, pyH), 7.11 (1H, d, pyH), 7.14 (1H, d, pyH), 7.20 (1H, d, pyH), 7.51 (1H, t, pyH), 7.60 (1H, t, pyH), 8.53 (1H, d, et-pyH). FAB-MS: *m*/*z* 228 $[MH]^+$.

The amounts of Me_2-etpy and Me-etpy were determined by ^1H NMR of the mixture of products by addition of a known amount of 2,6-dimethyl-1,4-benzoquinone as an internal standard. The presence of 6-methylpyridine-2-aldehyde was also confirmed by ^1H NMR. Total amounts of Me_2-etpy and Me-etpy recovered were 91 ± 3% for three experiments. Yields of Me-etpy were 42 ± 2%, which corresponds to 84 ± 4% based on **1**-oxo dimer, since **1**-oxo oxidizes one of two Me_2-etpy.

Thermal decomposition of **1** in acetone at room temperature under O_2 yielded a hydroxylated ligand (Me-etpy-CH_2OH) at a methyl position of Me_2-etpy in addition to Me-etpy and Me_2-etpy. The total recovery was ca. 92 ± 3%. Yields of Me-etpy-CH_2OH, Me-etpy, and Me_2-etpy were ca. 11 ± 3, 21 ± 3, and 60 ± 3%. The total oxidation yield of the ligand based on a dimer is 64%. ^1H NMR for Me-etpy-CH_2OH ($CDCl_3$, 400 MHz): δ(ppm) = 2.52 (3H, s, CH_3), 3.03 (4H, m, CH_2CH_2), 3.87 and 3.89 (4H, s, CH_2-py-Me and CH_2-py-CH_2OH), 4.72 (2H, s, -CH_2OH), 6.99 (1H, d, pyH), 7.06 (1H, d, pyH), 7.11 (2H, m, pyH), 7.18 (1H, d, pyH), 7.23 (1H, d, pyH), 7.48 (1H, t, pyH), 7.56 (2H, m, pyH), 8.49 (1H, d, et-pyH). FAB-MS: *m*/*z* 349 $[MH]^+$.

X-ray Crystallography. General Procedures. Data collections were carried out on a Rigaku/MSC Mercury diffractometer with

Table 1. Crystallographic Data for $[Cu(Me_2\text{-etpy})]ClO_4$ ($\mathbf{1}\cdot ClO_4$), $[Cu_2(O)_2(d_4\text{-}Me_2\text{-etpy})_2](ClO_4)_2\cdot 7(CH_3)_2CO$ ($\mathbf{1}\text{-}d_4\text{-oxo}\cdot ClO_4$), and $[Cu_2(Me_2\text{-etpy})_2(OMe)_2](ClO_4)_2\cdot 2CH_3OH$ ($\mathbf{1}\text{-OMe}\cdot ClO_4$)

	$\mathbf{1}\cdot ClO_4$	$\mathbf{1}\text{-}d_4\text{-oxo}\cdot ClO_4$	$\mathbf{1}\text{-OMe}\cdot ClO_4$
formula	$C_{21}H_{24}O_4\text{-}N_4CuCl$	$C_{63}H_{90}O_{17}N_8\text{-}Cu_2Cl_2$	$C_{46}H_{62}O_{12}N_8\text{-}Cu_2Cl_2$
temp, °C	−150	−150	−150
MW	495.44	1429.45	1117.04
cryst syst	monoclinic	triclinic	monoclinic
space group	$C2/c$	$P\bar{1}$	$P2_1/c$
a, Å	20.305(4)	10.910(4)	11.642(3)
b, Å	12.705(2)	11.259(4)	16.689(4)
c, Å	16.867(3)	14.986(5)	12.885(4)
α, deg		82.38(2)	
β, deg	100.123(7)	71.48(2)	97.700(6)
γ, deg		84.69(2)	
V, Å^3	4283(1)	1727(1)	2480(1)
Z	8	1	2
$2\theta_{max}$	55.0	55.0	55.0
F(000)	2048.00	752.00	1164.00
D_{calcd}, g/cm^3	1.536	1.374	1.495
abs coeff, cm^{-1}	11.81	7.64	10.34
no. of reflns collcd	17852	9787	20149
no. of indep reflns	3777 ($I \geq 3.00\sigma(I)$)	7330 ($I \geq 0.00\sigma(I)$)	4115 ($I \geq 3.00\sigma(I)$)
no. of refined params	280	397	316
GOF indication	1.38	1.21	1.11
largest peak/hole, e Å^{-3}	0.69/−0.98	1.56/−1.46	0.55/−0.54
R	0.044^a	0.118^b (0.092)^c	0.033^a
$R_w{}^d$	0.064	0.123	0.044

^{a} $R = \Sigma[|F_o| - |F_c|]/\Sigma|F_o|$ ($I \geq 3.0\sigma(I)$). ^{b} $R = \Sigma[|F_o| - |F_c|]/\Sigma|F_o|$ ($I \geq 0.0\sigma(I)$). ^{c} $R_w = \Sigma[|F_o| - |F_c|]/\Sigma|F_o|$ ($I \geq 2.0\sigma(I)$). ^{d} $R_w = [\Sigma w(|F_o| - |F_c|)^2/\Sigma w|F_o|^2]^{1/2}$; $w = 1/[\sigma^2(F_o) + p^2|F_o|^2/4]$ ($p = 0.068$ for $\mathbf{1}\cdot ClO_4$, $p = 0.068$ for $\mathbf{1}\text{-}d_4\text{-oxo}\cdot ClO_4$, and $p = 0.053$ for $\mathbf{1}\text{-OMe}\cdot ClO_4$).

graphite monochromated Mo Kα radiation ($\lambda = 0.71070$ Å). The data were collected at −150 ± 1 °C to a maximum 2θ value of 55.0°. A total of 720 oscillation images were collected. A first sweep of data was done using ω scans from −80.0 to 100.0° in 0.50° step, at $\chi = 45.0°$ and $\phi = 0.0°$. A second sweep of data was made using ω scans from −80.0° to 100.0° in 0.50° steps, at $\chi = 45.0°$ and $\phi = 90.0°$. Crystal-to-detector distances were 35 mm, and detector swing angles were 10°. Exposure rates were 10.0, 30.0, 40.0 s/deg for $\mathbf{1}\cdot ClO_4$, $\mathbf{1}\text{-}d_4\cdot ClO_4$, and $\mathbf{1}\text{-OMe}\cdot ClO_4$, respectively. The data were corrected for Lorentz and polarization effects. Empirical absorption corrections were applied.

The structures were solved by a direct method (SIR92)[24] and expanded using a Fourier technique.[25] The structures were refined by a full-matrix least-squares method by using the teXsan[26] crystallographic software package (Molecular Structure Corporation). The structure refinement of $\mathbf{1}\text{-}d_4\text{-oxo}\cdot ClO_4$ was carried out by all observations ($I > 0.0\sigma(I)$) to raise the reflection/parameter ratio. The other refinements were carried out by the observations ($I > 3.0\sigma(I)$). Non-hydrogen atoms, except for those of solvent molecules, were refined with anisotropic displacement parameters. Hydrogen atoms were positioned at calculated positions (0.95 Å). They were included, but not refined, in the final least-squares cycles. Crystallographic data are summarized in Table 1. Tables of final atomic coordinates, thermal parameters, and full bond distances and angles are given in Supporting Information (CIF).

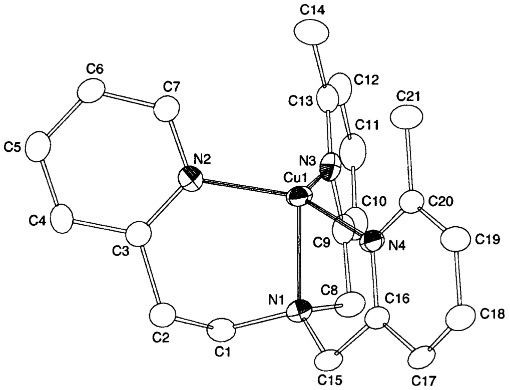

Figure 1. ORTEP view (50% probability) of a complex cation of $[Cu(Me_2\text{-etpy})]ClO_4$ ($\mathbf{1}\cdot ClO_4$). Hydrogen atoms are omitted for clarity.

$[Cu(Me_2\text{-etpy})]ClO_4$ ($\mathbf{1}\cdot ClO_4$). A single crystal with approximate dimensions 0.45 × 0.30 × 0.15 mm^3 was mounted on the tip of a glass rod. The asymmetric unit consists of one $[Cu(Me_2\text{-etpy})]^+$ cation and one perchlorate. The final R and R_w values were 0.044 and 0.064, respectively. The maximum peak on a final difference Fourier map was 0.69 e Å^{-3}.

$[Cu_2(O)_2(d_4\text{-}Me_2\text{-etpy})_2](ClO_4)_2\cdot 7(CH_3)_2CO$ ($\mathbf{1}\text{-}d_4\text{-oxo}\cdot ClO_4$). A single crystal with dimensions 0.25 × 0.17 × 0.10 mm^3 was picked up from a solution by a nylon loop (Hampton Research Co.) on a handmade cold copper plate mounted inside a liquid N_2 Dewar vessel at ca. −80 °C, and dipped quickly in liquid nitrogen. Then the dipped crystal was mounted on a goniometer head in a N_2 cryostream. There are a half of di(μ-oxo)dicopper(III) cation, one perchlorate, and seven acetone molecules with half occupations in an asymmetric unit. The final R and R_w values were 0.118 and 0.123 ($I \geq 0.0\sigma(I)$), respectively. The maximum peak on a final difference Fourier map (1.56 e Å^{-3}) was observed in the neighborhood of the perchlorate.

$[Cu_2(OMe)_2(Me_2\text{-etpy})_2](ClO_4)_2\cdot 2CH_3OH$ ($\mathbf{1}\text{-OMe}\cdot ClO_4$). A single crystal with approximate dimensions 0.25 × 0.10 × 0.05 mm^3 was picked up from the reaction solution on a handmade cold copper plate mounted inside a liquid N_2 Dewar vessel at −80 °C, and mounted on the top of a glass fiber. An asymmetric unit consists of a half of di(μ-methoxo)dicopper(II) cation, one perchlorate, and a methanol molecule. The final R and R_w values were 0.033 and 0.044, respectively. The maximum peak on a final difference Fourier map was 0.55 e Å^{-3}.

Results

Characterization of a Copper(I) Complex 1. The reaction of the tetradentate tripodal ligand Me_2-etpy with $[Cu(CH_3CN)_4]^+$ in ethanol under N_2 atmosphere gave a copper(I) complex $[Cu(Me_2\text{-etpy})]^+$ (**1**). Solid sample is air-stable for a few hours.

Figure 1 shows the structure of the complex cation of $\mathbf{1}\cdot ClO_4$, and the selected bond distances and angles are given in Table 2. The complex cation has a distorted trigonal pyramidal structure with three pyridyl nitrogens in the trigonal plane and tertiary amine nitrogen in the apex. The structure is similar to that of a closely related copper(I) complex having a pmea (bis(2-pyridylmethyl)(2-pyridylethyl)amine),[27] $[Cu(pmea)]^+$ (**6**), which has no 6-methyl substituent on the pyridyl group, and those of the copper(I) complexes having tetradentate tripodal ligands.[28−30] The

---

(24) *SIR-92*: Altomare, A.; Cascarano, G.; Giacovazzo, C.; Guagliardi, A.; Burla, M. C.; Polidori, G.; Camalli, M. *J. Appl. Crystallogr.* **1994**, *27*, 435.

(25) Beurskens, P. T.; Admiraal, G.; Beurskens, G.; Bosman, W. P.; de Gelder, R.; Israel, R.; Smits, J. M. M. *The DIRDIF-94 program system*; Technical Report of the Crystallography Laboratory; University of Nijmegen: The Netherlands, 1994.

(26) *teXsan: Crystal Structure Analysis Package*; Molecular Structure Corporation: The Woodlands, TX, 1985 and 1992.

Table 2. Selected Bond Distances and Angles of [Cu(Me_2-etpy)]ClO_4 (**1**·ClO_4), [$Cu_2(O)_2$(d_4-Me_2-etpy$)_2$]$(ClO_4)_2$·7$(CH_3)_2CO$ (**1**-d_4-oxo·ClO_4), and [$Cu_2(OMe)_2$(Me_2-etpy$)_2$]$(ClO_4)_2$·2CH_3OH (**1**-OMe·ClO_4)

	1·ClO_4	**1**-d_4-oxo·ClO_4	**1**-OMe·ClO_4
	Bond Lengths (Å)		
Cu1−N1	2.163(3)	2.003(3)	2.263(2)
Cu1−N2	1.989(3)	1.979(5)	2.029(2)
Cu1−N3	2.047(3)	2.412(4)	2.026(2)
Cu1−N4	1.995(3)	2.592(4)	
Cu1−O1		1.835(4)	1.940(2)
Cu1−O1*		1.832(3)	1.940(2)
Cu1···Cu2		2.866(1)	3.069(1)
O1···O1*		2.287(5)	2.375(2)
	Bond Angles (deg)		
N1−Cu1−N2	102.2(1)	99.2(2)	80.02(8)
N1−Cu1−N3	83.8(1)	78.1(2)	81.00(8)
N1−Cu1−N4	82.38(10)	74.0(1)	
N2−Cu1−N3	112.65(10)	86.4(2)	94.85(8)
N2−Cu1−N4	125.6(1)	91.4(2)	
N3−Cu1−N4	121.7(1)	151.3(1)	
Cu1−O1−Cu1*		102.8(2)	104.53(7)
O1−Cu1−O1*		77.2(2)	75.47(7)

average Cu−N_{eq} bond distance (2.010 Å) of **1**·ClO_4 is comparable to those of [Cu(pmea)]$^+$ (**6**: 1.98 Å),[27] [Cu(Me_2-tpa)]$^+$ (**4**: 2.008 Å),[11] [Cu(Me_3-tpa)]$^+$ (**5**: 2.01 Å),[12] [Cu(TMQA)]$^+$ (2.010 and 2.007 Å),[29] and [Cu(Ph_3tren)]$^+$ (2.01 Å).[30] Thus, introduction of 6-methyl groups into pyridyl groups has no significant influence on the in-plane Cu−N(6-methylpyridyl) bond distances in these copper(I) complexes. This is in contrast to the significant elongation of the M−N(6-methylpyridyl) bond distance due to steric hindrance between the methyl group(s) and an adjacent coordinated atoms in more sterically crowded five- and six-coordinate complexes.[31−34] The in-plane N−Cu−N bond angles of **1**·ClO_4 are in the range 112.65(10)−125.6(1)°, whereas those of **6** are in the range 101.6(5)−133.4(5)°.

Redox Behavior. The cyclic voltammogram of **1** in acetonitrile showed a quasireversible redox couple given in Figure S3 in Supporting Information. $E_{1/2}$(Cu(II)/Cu(I)) values of **1** and some other complexes are given in Table 3, which are approximate measures of the redox potentials. Table 3 shows that the replacement of the 2-pyridylmethyl group by the 2-pyridylethyl group and/or introduction of 6-methyl group into the pyridyl group causes a significant positive shift of the $E_{1/2}$(Cu(II)/Cu(I)) value. The $E_{1/2}$(Cu(II)/Cu(I)) value of **1** is 0 mV (ΔE = 175 mV) versus Ag/$AgNO_3$ in CH_3CN, which is 140 mV positive compared to that of **4** bearing a 2-pyridylmethyl pendant forming a five-membered chelate ring (Table 3). Such a significant positive shift is in line with the general trend that redox potentials of copper complexes having six-membered chelate ring(s) are more positive than those of complexes containing five-membered chelate ring(s) due to the stabilization of the copper(I) species and/or destabilization of the copper(II) species.[35] A similar observation was also made for the copper(II) complexes of TMPA and pmea,[27] the latter of which has also a 2-pyridylethyl pendant. Such redox properties have substantial influence on the dioxygen reactivity of the copper(I) complexes as well as stereochemistry of the complexes (vide infra).

Table 3. Electrochemical Data for Copper(I) Complexes in CH_3CN

complex	$E_{1/2}$(II/I) (ΔE) mV vs Ag/$AgNO_3$
[Cu(TMPA)(CH_3CN)]$^+$ (**2**)	−320 (105)
[Cu(Me-tpa)]$^+$ (**3**)	−260 (100)
[Cu(Me_2-tpa)]$^+$ (**4**)	−140 (100)
[Cu(d_4-Me_2-etpy)]$^+$ (**1**)	0 (175)
[Cu(Me_3-tpa)]$^+$ (**5**)	70 (105)^a

^{a} Ref 12.

Dioxygen Reactivity of Copper(I) Complexes 1 and 1-d_4. Complex **1** gradually reacted with dioxygen in acetone at room temperature under 1 atm of O_2 to give a green species, whereas it reacted very slowly with dioxygen at −80 °C to give a brown species [$Cu_2(O)_2$(Me_2-etpy$)_2$]$^{2+}$ (**1**-oxo). The electronic spectrum of **1**-oxo showed absorption maxima at 526 and ~765 nm. Monitoring the electronic spectral change indicated that the formation of **1**-oxo was very slow at −80 °C (it took more than 4 h to reach maximum absorbance at 526 and ~765 nm), and during the formation, some decomposition occurred simultaneously as shown in Figure S4 in Supporting Information. The thermal decomposition of **1**-oxo resulted in *N*-dealkylation of the Me_2-etpy ligand (vide infra). However, deuteration of four hydrogen atoms of the methylene groups of the Me_2-etpy ligand leads to a significant stabilization of [$Cu_2(O)_2$(d_4-Me_2-etpy$)_2$]$^{2+}$ (**1**-d_4-oxo). The electronic spectrum of **1**-d_4 also shows absorption bands at 526 nm and ~765 nm in acetone at −80 °C under 1 atm of O_2 as shown in Figure 2b. The brown species **1**-d_4-oxo is stable for days under the conditions. The intensity of the absorption band at 526 nm is not linearly dependent on the concentration of the complex, suggesting the presence of an equilibrium between **1**-d_4 and **1**-d_4-oxo which is not fully formed under the conditions. The electronic spectrum (d) in Figure 2 also shows a shoulder at ~380 nm, and Gaussian analysis of the spectrum (inset in Figure 2) suggests the presence of a band at 389 nm (25713 cm^{-1}), whose intensity is also dependent on the concentration of **1**-d_4.

---

(27) Schatz, M.; Becker, M.; Thaler F.; Hampel, F.; Schindler, S.; Jacobson, R. R.; Tyeklár, Z.; Murthy, N. N.; Ghosh, P.; Chen, Q.; Zubieta, J.; Karlin, K. D. *Inorg. Chem.* **2001**, *40*, 2312.

(28) (a) Halfen, J. A.; Young, V. G. Jr.; Tolman, W. B. *J. Am. Chem. Soc.* **1996**, *118*, 10920. (b) Berreau, L. M.; Halfen, J. A.; Young, V. G., Jr.; Tolman, W. B. *Inorg. Chim. Acta* **2000**, *297*, 115.

(29) Wei, N.; Murthy, N. N.; Chen, Q.; Zubieta, J.; Karlin, K. D. *Inorg. Chem.* **1994**, *33*, 1953.

(30) Alyea, E. C.; Ferguson, G.; Jennings, M. C.; Xu, Z. *Polyhedron* **1990**, *9*, 739.

(31) (a) Goodson, P. A.; Hodgson, D. J. *Inorg. Chem.* **1989**, *28*, 3606. (b) Goodson, P. A.; Oki, A. R.; Glerup, J.; Hodgson, D. J. *J. Am. Chem. Soc.* **1990**, *112*, 6248.

(32) Nagao, H.; Komeda, N.; Mukaida, M.; Suzuki, M.; Tanaka, K. *Inorg. Chem.* **1996**, *35*, 6809.

(33) Zang, Y.; Kim, J.; Dong, Y.; Wilkinson, E. C.; Appelman, E. H.; Que, L., Jr. *J. Am. Chem. Soc.* **1997**, *119*, 4197.

(34) (a) Hayashi, Y.; Kayatani, T.; Sugimoto, H.; Suzuki, M.; Inomata, K.; Uehara, A.; Mizutani, Y.; Kitagawa, T.; Maeda, Y. *J. Am. Chem. Soc.* **1995**, *117*, 11220. (b) Shiren, K.; Ogo, S.; Fujinami, S.; Hayashi, H.; Suzuki, M.; Uehara, A.; Watanabe, Y.; Moro-oka, Y. *J. Am. Chem. Soc.* **2000**, *122*, 254. (c) Shiren, K.; Fujinami, S.; Suzuki, M.; Uehara, A. *Inorg. Chem.* **2002**, *41*, 1598.

(35) Ambundo, E. A.; Deydier, M.-V.; Grall, A. J.; Aguera-Vega, N.; Dressel, L. T.; Cooper, T. H.; Heeg, M. J.; Ochrymowycz, L. A.; Rorabacher, D. B. *Inorg. Chem.* **1999**, *38*, 4233.

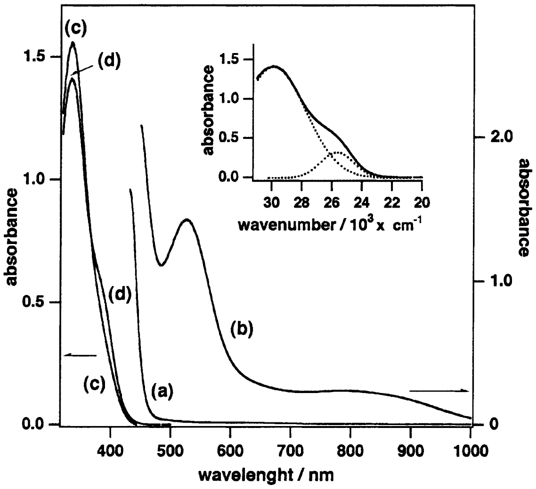

Figure 2. Electronic spectra of (a) **1**-d_4 (9.8 mM) in acetone at −80 °C under N_2 and (b) under 1 atm of O_2 measured by an optical fiber with a light path length of 1.11 cm, and (c) **1**-d_4 (1.48 mM) at −80 °C under N_2 and (d) under 1 atm of O_2 with 1 mm cell. Inset: Gaussian analysis of the spectrum (d) in 300−450 nm region.

Characterization of a Bis(μ-oxo)dicopper(III) Complex 1-d_4-oxo. The deuterated ligand d_4-Me$_2$-etpy significantly stabilized the bis(μ-oxo)dicopper(III) complex $[Cu_2(O_2)(d_4\text{-}Me_2\text{-}etpy)_2]^{2+}$ (**1**-d_4-oxo), which was successfully crystallized from an acetone solution as orange-brown crystals by the addition of *n*-hexane into the solution. X-ray crystallography shows that the complex cation consists of a centrosymmetric $Cu_2(\mu\text{-}O)_2$ core with the d_4-Me$_2$-etpy nitrogens (Figure 3a). Each copper ion has an axially elongated octahedral structure composed of a N_4O_2 donor set having a pyridylethyl pendant in a basal plane and two 6-methyl-2-pyridylmethyl ones which interact weakly with each copper ion in the axial positions (2.412(4) and 2.592(4) Å), similar to those of $[Cu_2(O_2)(Me_2\text{-}tpa)_2]^{2+}$ **4**-oxo (2.48(1) and 2.55(1) Å).[11] The average Cu−O (1.834 Å) and Cu···Cu′ (2.866(1) Å) distances are slightly longer than those of the bis(μ-oxo)dicopper(III) complexes, $[Cu_2(O)_2(Bn_3\text{-}tacn)_2]^{2+}$ (**7**-oxo; 1.806 and 2.794 Å),[15a,b] $[Cu_2(O)_2(L_{ME})_2]^{2+}$ (**8**-oxo; 1.806 and 2.743 Å),[16] $[Cu_2(O)_2(Me_2\text{-}tpa)_2]^{2+}$ (**4**-oxo: 1.803 and 2.758(4) Å),[11] but slightly shorter than those of $[Cu_2(O)_2(Bu^t{}_2P(NSiMe_3)_2)_2]^{2+}$ (1.865 and 2.906(1) Å).[36]

Thermal decomposition of **1** in methanol under O_2 atmosphere at room temperature afforded blue single crystals as well as ligand modification. X-ray crystallography of a blue crystal revealed that the complex is a bis(μ-OMe)dicopper(II) complex ($[Cu_2(OMe)_2(Me_2\text{-}etpy)_2](ClO_4)_2{\cdot}2CH_3OH$ (**1**-OMe·ClO_4)) as shown in Figure 3b. Unlike **1**-d_4-oxo, each copper ion has a distorted square pyramidal structure, where the tertiary amine nitrogen is in the apical position and two 6-methylpyridyl pendants form a square plane with bridging methoxides. Consequently, one pyridylethyl pendant is free from coordination.

As mentioned above, the electronic spectrum of **1**-d_4-oxo showed three absorption bands (~390, 526, and ~765 nm) in the UV−vis region which are similar to those of **4**-oxo (378 nm (ϵ = ~19000 M^{-1} cm^{-1}), ~490 nm (ϵ = ~330 M^{-1} cm^{-1}), and 784 nm (ϵ = ~60 M^{-1} cm^{-1}))[11] and **5**-d_{15}-oxo (~390, 517, and ~810 nm).[12] The absorption band at ~390 nm observed for **1**-d_4-oxo can be assigned to the oxo-to-copper(III) (LMCT) transition.[37] Thus, the transition energies of the complexes having tetradentate tripodal ligands are higher than those of the bis(μ-oxo)dicopper(III) complexes containing tridentate and bidentate supporting ligands reported so far (390−448 nm).[11,21,37,38] It should be noted that the complexes having tetradentate tripodal ligands have weak absorption bands at ~500 and 700−800 nm. There is a possibility that the absorption bands are attributable to the other species such as (μ-η^2:η^2-peroxo)dicopper(II) species. In order to confirm that the absorption bands at 526 and ~765 nm in acetone are ascribed to the bis(μ-oxo)dicopper(III) species **1**-d_4-oxo, the reflectance spectra of a powdered sample prepared from crystals were measured at ca. −110 °C (Figure 4). The reflectance spectra also showed three bands at ~380, ~520, and ~770 nm, which are almost the same as those measured in acetone. The results definitively confirmed that these three bands are attributable to the electronic transitions of **1**-d_4-oxo. The presence of such visible bands was confirmed for the first time for bis(μ-oxo)dicopper(III) species.

The resonance Raman spectrum of **1**-d_4-oxo measured in acetone (~1 mM) at −80 °C under O_2 atmosphere with a 406.7 nm laser excitation showed an isotope-sensitive band at 579 cm^{-1} with $^{16}O_2$ (551 cm^{-1} with $^{18}O_2$) as shown in Figure 5, characteristic of those observed for the bis(μ-oxo)dicopper(III) complexes.[37,38] There are additional isotope-sensitive bands at 1158 cm^{-1} with $^{16}O_2$ and 1102 cm^{-1} with $^{18}O_2$, which can be assigned to the overtones of the 579 and 551 cm^{-1} bands, respectively. A similar observation has been also made for the bis(μ-oxo)dicopper(III) complex having a L_{ME} ligand.[37] No observation of the O−O stretching vibration at 720−765 cm^{-1} and the Cu−Cu stretching vibration at ~300 cm^{-1} attributable to a (μ-η^2:η^2-peroxo)dicopper(II) species[38] was made under the experimental conditions. The results are in line with the electronic spectral results.

Figure 6 shows ^{1}H NMR spectra of **1**-d_4 ([Cu] = 19.0 mM) in d_6-acetone under N_2 atmosphere (a) and under O_2 (b) at −80 °C. The spectrum b clearly exhibits two sets of sharp signals attributable to **1**-d_4 and **1**-d_4-oxo, indicating that **1**-d_4-oxo is diamagnetic and not fully formed. The methyl proton signal of **1**-d_4 at 3.03 ppm is upfield shifted upon oxygenation and splits into two signals at 1.22 and 1.82 ppm. Unlike the ethylene protons of **1**-d_4 (3.18 and 3.29 ppm), those of **1**-d_4-oxo appear as two doublets at 3.10 and 2.91 ppm and two multiplets at 2.80 and 2.36 ppm, indicating that the conformational change of the in-plane 2-pyridylethylamine chelate ring is locked within the NMR time scale, leading to nonequivalence of two methyl protons on the pyridyl groups in the axial positions. The upfield shift of two methyl protons may be due to the ring current effect of

---

(36) Straub, B. F.; Rominger, F.; Hofmann, P. *Chem. Commun.* **2000**, 1611.

(37) Henson, M. J.; Mukherjee, P.; Root, D. E.; Stack, T. D. P.; Solomon, E. I. *J. Am. Chem. Soc.* **1999**, *121*, 10332.

(38) Holland, P. L.; Cramer, C. J.; Wilkinson, E. C.; Mahapatra, S.; Rodgers, K. R.; Itoh, S.; Taki, M.; Fukuzumi, S.; Que, L., Jr.; Tolman, W. B. *J. Am. Chem. Soc.* **2000**, *122*, 792.

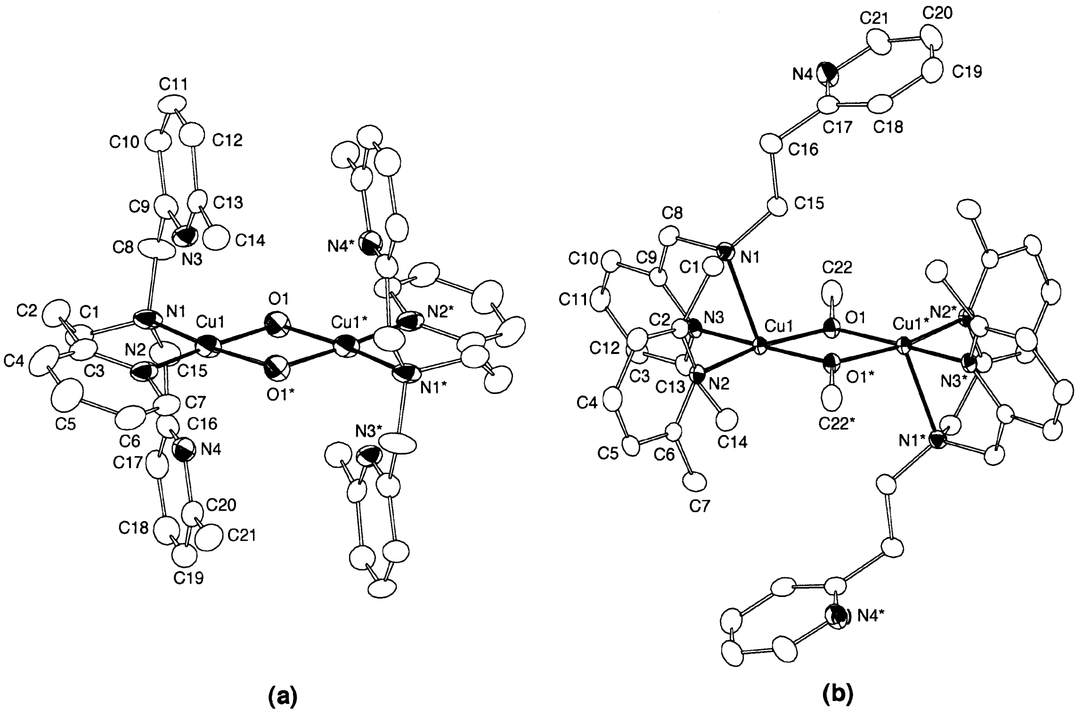

Figure 3. ORTEP views (50% probability) of complex cations of (a) $[Cu_2(O)_2(d_4\text{-}Me_2\text{-}etpy)_2](ClO_4)_2 \cdot 7(CH_3)_2CO$ (**1**-*d*$_4$-oxo·ClO$_4$), and (b) $[Cu_2(OMe)_2(Me_2\text{-}etpy)_2](ClO_4)_2 \cdot 2CH_3OH$ (**1**-OMe·ClO$_4$). Hydrogen atoms are omitted for clarity.

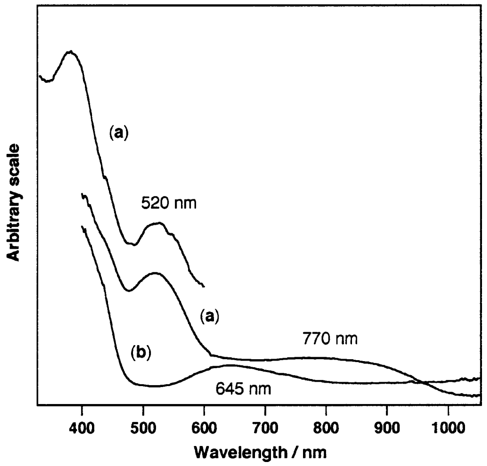

Figure 4. Reflectance spectra of a powdered sample of **1**-*d*$_4$-oxo·ClO$_4$ (a) at ca. −110 °C and that of the sample decomposed at room temperature (b) measured at ca. −110 °C.

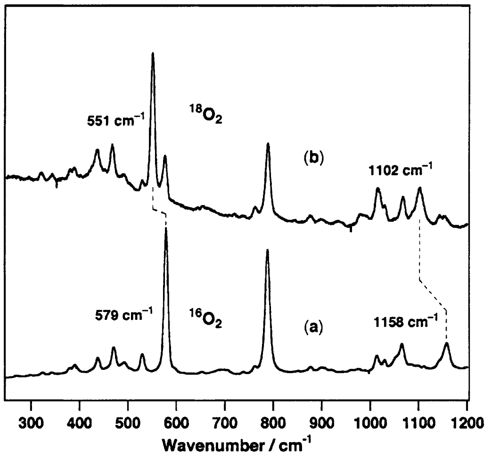

Figure 5. Resonance Raman spectra of **1**-*d*$_4$-oxo in acetone (ca. 1 mM) at −80 °C prepared by $^{16}O_2$ (a) and $^{18}O_2$ (b) with 406.7 nm laser excitation.

two 6-methylpyridyl groups faced with the methyl groups as can be seen in Figure 3. Such an upfield shift of methyl protons is also observed for $[Cu_2(O)_2(Me_2\text{-}tpa)_2]^{2+}$ (**4**-oxo). The distances between the pyridyl rings and the methyl groups in **1**-*d*$_4$-oxo are 3.45 and 3.53 Å, and those in **4**-oxo are 3.60 and 3.65 Å. Integration of the methyl signals revealed that 70% of **1**-*d*$_4$ is converted to **1**-*d*$_4$-oxo under the above conditions, although **4**-oxo is fully formed in *d*$_6$-acetone at −70 °C under 1 atm of O$_2$,[10] indicating that the oxygenation of **4** is higher than that of **1**-*d*$_4$.

Interconversion between the Copper(I) Complex 1-*d*$_4$ and the Bis(μ-oxo)dicopper(III) Complex 1-*d*$_4$-oxo. Significant stabilization of **1**-*d*$_4$-oxo allowed the estimation of the equilibrium constants at various temperatures. Figure 7 shows the electronic spectral change of **1**-*d*$_4$ in acetone under O$_2$ atmosphere depending on the temperature change from −80 to −55 °C. As the temperature increases, the absorption intensity decreases. The spectrum (g) measured by rechilling the solution at −80 °C after repetition of the cycle shows no appreciable decomposition. Thus, a reversible oxygenation−deoxygenation cycle can be achieved by changing the temperatures, whereas deoxygenation by purging with N$_2$ at −80 °C was very slow and it was difficult to complete the deoxygenation at −80 °C. The spectral change is well interpreted in terms of the following equilibrium.

$$2[Cu(d_4\text{-}Me_2\text{-}etpy)]^+ \ (\mathbf{1}\text{-}d_4) + O_2 \overset{K}{\rightleftharpoons} [Cu_2(O)_2(d_4\text{-}Me_2\text{-}etpy)_2]^{2+} \ (\mathbf{1}\text{-}d_4\text{-oxo}) \quad (1)$$

The equilibrium constants (*K*'s) in acetone at −80 °C determined independently by two methods, electronic spec-

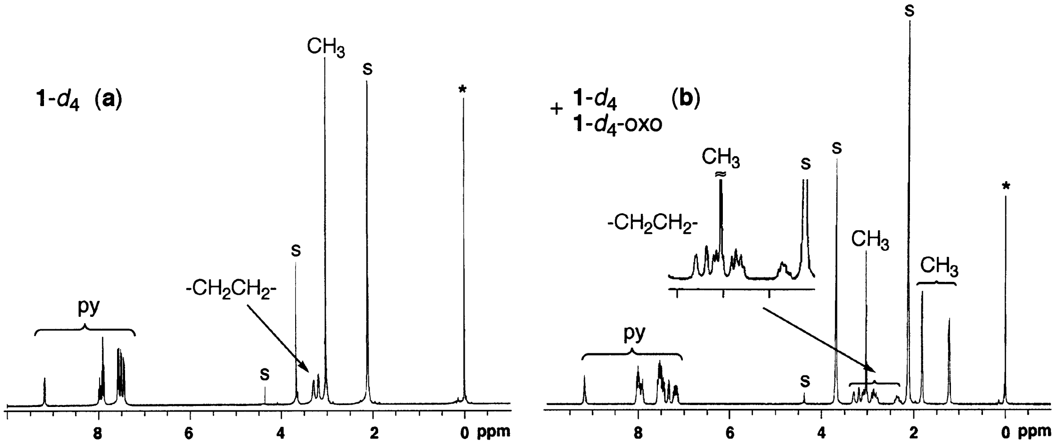

Figure 6. ^{1}H NMR spectra of **1**-d_4 ([Cu] = 19.0 mM) in d_6-acetone under N_2 (a) and under O_2 (b) at −80 °C. The signals marked with s and * are the solvent and TMS signals, respectively.

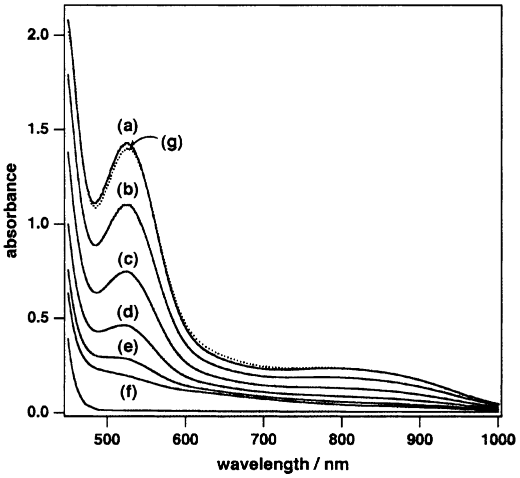

Figure 7. Electronic spectral change of **1**-d_4 in d_6-acetone ([Cu] = 9.8 mM) under O_2 ([O_2] = 5.106 mM) depending on the temperatures measured by an optical fiber with a light path length of 1.11 cm: −80 °C (a), −75 °C (b), −70 °C (c), −65 °C (d), −60 °C (e), −55 °C (f), −80 °C (rechilled after measurement at −55 °C) (g, ···).

trophotometric and NMR measurements, gave good agreement each other (see the Experimental Section). The results are given in Table 4 together with thermodynamic parameters for oxygenation for some other copper(I) complexes.[12,21,39−41] Oxygenation of **1**-d_4 is about 5 times higher than that of [Cu(d_{15}-Me$_3$-tpa)]$^+$ (**5**-d_{15}) in acetone at −80 °C,[12] whereas it is lower than that of **4** as mentioned in NMR results. Enthalpy and entropy changes are -53 ± 2 kJ mol^{-1} and -187 ± 10 J mol^{-1} K^{-1}, respectively, which are quite different from those of a bis(μ-oxo)dicopper(III) complex ([Cu(AN)]$^+$ (**9**)) having a linear aliphatic triamine ligand reported by Karlin et al. (Table 4).[21] Oxygenation of **1**-d_4 is significantly lower than that of **9**, probably due to the greater stabilization of the copper(I) oxidation state of **1**-d_4.

Reactivity of 1-d_4-oxo. Although complex **1**-oxo in acetone was not fully formed even at −80 °C under O_2 atmosphere, it decomposed to give a blue-green solution. A ligand recovery experiment revealed that *N*-dealkylation of the ligand occurs to give (6-methyl-2-pyridylmethyl)(2-pyridylethyl)amine (Me-etpy) in yield of more than 80% based on a dimer. The presence of 6-methylpyridine-2-aldehyde was also identified by GC-MS and NMR. Significant thermal stabilization of **1**-d_4-oxo implies that the ligand modification of **1**-d_4-oxo proceeds via the C−H bond cleavage of the methylene groups of Me$_2$-etpy as found for various bis(μ-oxo)dicopper(III) complexes. Thus, **1**-oxo has a regioselective monooxygenase activity for the supporting ligand under the conditions as found for **4** having a Me$_2$-tpa ligand. In contrast, it was also found that thermal decomposition of **1** in acetone at room temperature under O_2 atmosphere resulted in partial hydroxylation of a methyl group and *N*-dealkylation of Me$_2$-etpy to give Me-etpy-CH$_2$OH (yield = ~10%) and Me-etpy (yield = ~20%), respectively, where the formation of **1**-oxo was not detected. Total oxidation yield of the ligand based on the dimer is ~60%, which is lower than that at −80 °C (~83%).

Discussion

Introduction of methyl group(s) into the 6-position of the pyridyl group(s) of the TMPA ligand has significant influence on the $E_{1/2}$(Cu(II)/Cu(I)) values of the copper(I) complexes ([Cu(Me$_n$-tpa)]$^+$ $n = 1-3$). As the number of methyl groups increases, the $E_{1/2}$(Cu(II)/Cu(I)) values of the copper(I) complexes result in a substantial positive shift as seen in Table 3, probably due to the stabilization of the copper(I) species and/or destabilization of the copper(II) species.[35] Furthermore, such modification has a significant influence on the dioxygen reactivity of the copper(I) complexes; [Cu(Me-tpa)]$^+$ forms a *trans*-(μ-1,2-peroxo)dicopper(II) species with a trigonal bipyramidal structure, whereas **1**-d_4, [Cu(Me$_2$-tpa)]$^+$ (**4**), and [Cu(d_{15}-Me$_3$-tpa)]$^+$ (**5**-d_{15}) gave bis(μ-oxo)dicopper(III) species, where two or three methyl groups seem to prevent the formation of a trigonal bipyramidal structure due to steric requirement. The ligands Me$_2$-tpa and d_4-Me$_2$-etpy facilitate reversible conversion between copper(I) and bis(μ-oxo)dicopper(III) species. Thus, sterically hindered tetradentate tripodal ligands have a unique ability to stabilize both copper(I) and copper(III)

---

(39) Jung. B.; Karlin, K. D.; Zuberbühler, A. D. *J. Am. Chem. Soc.* **1996**, *118*, 3763.

(40) Liang. H.-C.; Karlin, K. D.; Dyson, R.; Kaderli, S.; Jung, B.; Zuberbühler, A. D. *Inorg. Chem.* **2000**, *39*, 5884.

(41) Karlin, K. D.; Wei, N.; Jung, B.; Kaderli, S.; Niklaus, P.; Zuberbühler, A. D. *J. Am. Chem. Soc.* **1993**, *115*, 9506.

Table 4. Thermodynamic Parameters for Oxygenation Reactions of Various Copper(I) Complexes

complex	ΔH/kJ mol^{-1} ΔS/J mol^{-1} K^{-1}	T/K	K/M^{-2}	ref
	bis(μ-oxo)Cu(III)$_2$			
[Cu(d_4-Me$_2$-etpy)]$^+$ (**1**-d_4)	-53 ± 2 (ΔH)	193	$4.0 \pm 0.2 \times 10^4$	this work
	-187 ± 10 (ΔS)	198	$1.7 \pm 0.1 \times 10^4$	
		203	$7.0 \pm 0.2 \times 10^3$	
		208	$3.1 \pm 0.2 \times 10^3$	
		213	$1.6 \pm 0.2 \times 10^3$	
		218	$1.0 \pm 0.1 \times 10^3$	
[Cu(d_{15}-Me$_3$-tpa)]$^+$ (**5**-d_{15})		193	$\sim 3.8 \times 10^3$	12
[Cu(AN)]$^+$ (**9**)	-24 ± 1 (ΔH)	183	$1.02 \pm 0.07 \times 10^6$	21
	-14 ± 6 (ΔS)			
	(μ-η^2:η^2-peroxo)Cu(II)$_2$^{a}			
[Cu(MeAN)]$^+$	-28 ± 2 (ΔH)	183	$7.6 \pm 0.6 \times 10^4$	21
	-61 ± 12 (ΔS)			
[Cu$_2$(N$_4$)]$^{2+}$	-58.2 ± 2 (ΔH)	183	7×10^{7} ^{b}	39
	-165 ± 8 (ΔS)			
[Cu$_2$(N$_4$)(CH$_3$CN)$_2$]$^{2+}$	-84 ± 1 (ΔH)	183	8×10^{9} ^{b}	40
	-270 ± 5 (ΔS)			
	trans-(μ-1,2-peroxo)^a			
[Cu(TMPA)(RCN)]$^+$ (**2**)	-81 ± 3 (ΔH)	183	4.3×10^{11}	41
	-220 ± 11 (ΔS)			

^{a} $2\mathrm{Cu(I)} + \mathrm{O_2} \overset{K}{\rightleftharpoons} \mathrm{Cu_2(O_2)}$. ^{b} K/M^{-1}.

oxidation states: they can take not only a square planar structure with weak ligation from the axial positions which can fit to the copper(III) oxidation state, but also a trigonal pyramidal structure suitable for the copper(I) oxidation state. The relative stability of bis(μ-oxo)dicopper(III) species against copper(I) species is **4** > **1**-d_4 > **5**-d_{15}, which is well correlated with the $E_{1/2}$(Cu(II)/Cu(I)) values; as the $E_{1/2}$ value becomes negative, the copper(I) species becomes unstable, and the formation ratio of bis(μ-oxo)dicopper(III) species becomes more favorable.

It has been shown that, for many complexes having bidentate and tridentate ligand systems, there is equilibrium between (μ-η^2:η^2-peroxo)dicopper(II) and bis(μ-oxo)dicopper(III) species, and the relative stability between them is highly dependent on various factors such as electronic and steric effects as well as solvent, counterion, temperature, and so on.[3,4,15a,19−23] However, only bis(μ-oxo)dicopper(III) species formed for the complexes having the present type of the tetradentate tripodal ligands reported so far.[11,12,42] Thus, sterically hindered tetradentate tripodal ligands tend to form bis(μ-oxo)dicopper(III) species compared to those of bidentate and tridentate ligands.

The oxidation reactivity toward the supporting ligands in three bis(μ-oxo)dicopper(III) species, **1**-oxo, **4**-oxo, and **5**-oxo, is also dependent on the $E_{1/2}$(Cu(II)/Cu(I)) values and stereochemistry of the ligands. There is a tendency that relative reactivity of the above three bis(μ-oxo)dicopper(III) species toward the oxidation of the supporting ligands becomes higher as the $E_{1/2}$(Cu(II)/Cu(I)) values become positive (Table 3). Deuteration of the ligands (d_4-Me$_2$-etpy and d_{15}-Me$_3$-tpa), however, greatly stabilizes the bis(μ-oxo)dicopper(III) species, indicating that the rate determining step of the oxidation for the supporting ligands in these complexes is the C−H bond cleavage by the oxo groups.

The oxidation of the supporting ligands in the high-valent bis(μ-oxo)dimetal(III) complexes has also been shown to be highly dependent on the structure and the C−H bond energy.[3,15b,16,34b,43] The regioselective oxidation of the methylene group in **1**-oxo seems to reflect its structure and C−H bond energy as found for **4**-oxo (Figure 8). A Chem3D model of **1**-oxo suggested that the H···O$_{\mathrm{oxo}}$ distances of the methylene hydrogens of the 6-methyl-2-pyridylmethyl pendants in the apical positions and those of the methyl groups are ~2.4 and ~2.5 Å, respectively, which are slightly shorter than those of **4**-oxo (~2.64 and ~2.61 Å for the methylene and methyl groups), where the C−H bond distances are set to 1.10 Å. Regioselective hydrogen abstraction of the methylene group at low temperature is in line with the weaker C−H bond energy of the methylene group relative to that of the methyl group. For complex **5**-oxo, however, both the methyl and methylene hydrogens are oxidized. Although the structure of **5**-oxo is not available at present, the structure of the corresponding bis(μ-oxo)dinickel(III) complex ([Ni$_2$(O)$_2$(Me$_3$-tpa)$_2$)]$^{2+}$ (**10**)) suggests that there are in-plane methyl groups in **5**-oxo which must be closer to the oxo groups than those of the methylene hydrogens; this proximity effect seems to be responsible to the oxidation of the methyl group in **5**-oxo, although complex **10** reacts only with the methyl groups.

Conclusion. A sterically hindered tetradentate ligand, Me$_2$-etpy, forms a bis(μ-oxo)dicopper(III) complex **1**-oxo at low temperature as well as closely related ligands such as Me$_2$-tpa and Me$_3$-tpa. **1**-oxo has a monooxygenase activity toward the supporting ligand to cause *N*-dealkylation. Deuteration of the methylene hydrogens of 6-methyl-2-pyridylmethyl pendants of Me$_2$-etpy significantly stabilized the bis(μ-oxo)dicopper(III) species **1**-d_4-oxo. The electronic spectra showed

---

(42) Shimazaki, Y.; Nogami, T.; Tani, F.; Odani, A.; Yamauchi, O. *Angew. Chem., Int. Ed.* **2001**, *40*, 3859.

(43) Hikichi, S.; Yoshizawa, M.; Sasakura, Y.; Akita, M.; Moro-oka, Y. *J. Am. Chem. Soc.* **1998**, *120*, 10567−10568. Hikichi, S.; Yoshizawa, M.; Sasakura, Y.; Komatsuzaki, H.; Moro-oka, Y.; Akita, M. *Chem. Eur. J.* **2001**, *7*, 5011.

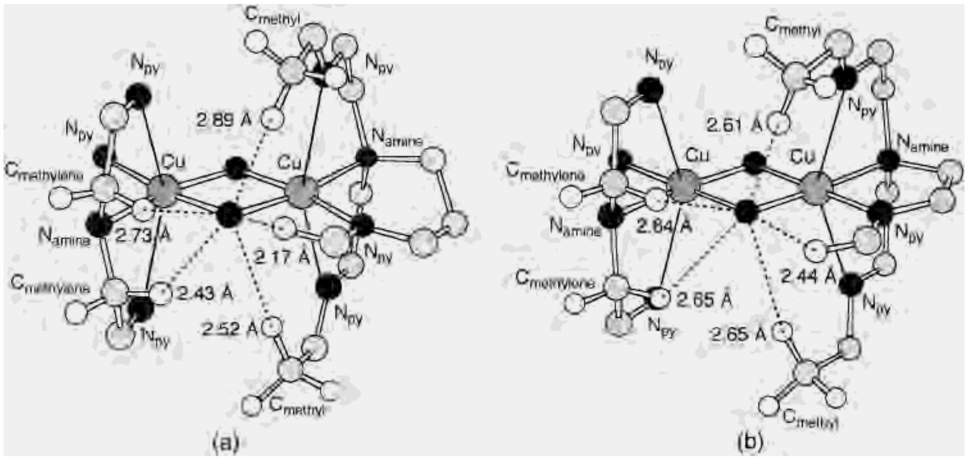

Figure 8. Chem3D views of **1**-*d*$_4$-oxo (a) and **4**-oxo (b) showing the H···O$_{oxo}$ distances close to the oxo groups. Hydrogen atoms were placed at the calculated positions and the C−H bond distances are set to 1.10 Å.

an LMCT (oxo to Cu(II)) band at ∼390 nm and two additional absorption bands at 526 and ∼765 nm, which may be assigned as LMCT and/or d−d transitions. Stabilization of **1**-*d*$_4$-oxo toward the oxidation of the supporting ligand indicates that the rate determining step of the *N*-dealkylation for the supporting ligand is the C−H bond cleavage of the methylene groups of 6-methyl-2-pyridylmethyl pendants in the axial positions. The crystal structure of **1**-*d*$_4$-oxo revealed that the H···O$_{oxo}$ distances of the methylene hydrogens of the 6-methyl-2-pyridylmethyl pendants in the apical positions and those of the methyl groups are comparable (∼2.4 to ∼2.5 Å). Regioselective hydrogen abstraction from the methylene groups at −80 °C is in line with the weaker C−H bond energy of the methylene group relative to that of the methyl group. In addition, reversible conversion between **1**-*d*$_4$ and **1**-*d*$_4$-oxo was also observed as the Me$_2$-tpa complex **4** (reversible four electron reduction of dioxygen by **1**-*d*$_4$ and four electron oxidation of the resulting oxo groups by **1**-*d*$_4$-oxo). Replacement of a 2-pyridylmethyl pendant of Me$_2$-tpa with a 2-pyridylethyl pendant greatly stabilizes a copper(I) species compared to Me$_2$-tpa and significantly shifts the equilibrium to the left-hand side in eq 1. Thus, the reactivity of the copper(I) complexes having a series of sterically hindered tetradentate tripodal ligands can be significantly modulated by modifying the stereochemistry of the pendant arm.

Acknowledgment. This work is supported by Grants-in-Aid for Scientific Research from the Ministry of Education, Science, and Culture, Japan (M.S. and T.K.).

Supporting Information Available: Figures S1−S4 and three X-ray crystallographic files in CIF format. This material is available free of charge via the Internet at http://pubs.acs.org.

IC0345166